Biomech Model Mechanobiol (2010) 9:117–125
DOI 10.1007/s10237-009-0165-2

ORIGINAL PAPER

Cyclic strain inhibits acute pro-inflammatory gene expression in aortic valve interstitial cells

Kathryn E. Smith · Scott A. Metzler · James N. Warnock

Received: 10 November 2008 / Accepted: 9 July 2009 / Published online: 28 July 2009

Abstract Mechanical in vitro preconditioning of tissue engineered heart valves is viewed as an essential process for tissue development prior to in vivo implantation. However, a number of pro-inflammatory genes are mechanosensitive and their elaboration could elicit an adverse response in the host. We hypothesized that the application of normal physiological levels of strain to isolated valve interstitial cells would inhibit the expression of pro-inflammatory genes. Cells were subjected to 0, 5, 10, 15 and 20% strain. Expression of VCAM-1, MCP-1, GM-CSF and OPN was then measured using qRT-PCR. With the exception of OPN, all genes were significantly up regulated when no strain was applied. MCP-1 expression was significantly lower in the presence of strain, although strain magnitude did not affect the expression level. VCAM-1 and GM-CSF had the lowest expression levels at 15% strain, which represent normal physiological conditions. These findings were confirmed using confocal microscopy. Additionally, pSMAD 2/3 and IκBα expression were imaged to elucidate potential mechanisms of gene expression. Data showed that 15% strain increased pSMAD 2/3 expression and prevented phosphorylation of IκBα. In conclusion, cyclic strain reduces expression of pro-inflammatory genes, which may be beneficial for the in vitro pre-conditioning of tissue engineered heart valves.

Keywords Heart valve · Cyclic strain · Inflammation · Tissue engineering · Interstitial cells

K. E. Smith · S. A. Metzler · J. N. Warnock (✉)
Department of Agricultural and Biological Engineering, Mississippi State University, 130 Creelman Street, Mississippi State, MS 39762, USA
e-mail: jwarnock@abe.msstate.edu

1 Introduction

The aortic valve, located between the left ventricle and the ascending aorta, is constantly subjected to an array of mechanical forces. These forces include shear stress, compression, tension and flexure (Butcher et al. 2008). Studies have shown that these stimuli are necessary to maintain homeostasis and correct functioning of the valve. Their absence results in a decrease in α-smooth muscle actin expression, significant changes in extra cellular matrix composition and altered DNA synthesis (Konduri et al. 2005; Weston and Yoganathan 2001). Consequently, it has long been accepted that in vitro biomimetic mechanical preconditioning greatly enhances the development of tissue engineered heart valves by increasing collagen and DNA content relative to static controls (Hoerstrup et al. 2002, 2000). However, mechanical stimuli are also known to be intrinsically involved in cardiovascular pathogenesis. It has recently been shown that deviations from normal physiological cyclic strain increases pro-inflammatory protein expression in aortic valve endothelial cells (AVEC) (Metzler et al. 2008). It is also known that elevated cyclic pressure can upregulate certain inflammatory genes in aortic valve interstitial cells (VIC) (Warnock et al. 2006).

Inflammation is generally defined as the reaction of vascularized living tissue to local injury. It sets in motion a series of events that may heal and reconstitute the implant site through replacement of the injured tissue by regeneration of native parenchymal cells, formation of fibrous scar tissue, or a combination of these two processes. The process is instigated by the presence of specific molecules that are responsible for adhesion, migration and accumulation of monocytes and T-cells. These include vascular cell adhesion molecules (VCAM) that act in conjunction with chemotactic molecules, such as monocyte chemotactic protein 1

(MCP-1), expressed by the endothelium and smooth muscle cells to attract monocytes and T-cells into the tissue. Monocytes migrate into the sub-endothelial space and differentiate into macrophages (Shahi et al. 1997). There are few, if any, neutrophils present in aortic valve lesions, as is the case with atherosclerosis (Mohler 2004). Monocyte derived macrophages are scavenging antigen-presenting cells, which secrete cytokines, chemokines, growth regulating factors and metalloproteinases. The continual entry and survival of monocytes depends in part, on the expression of macrophage colony stimulating factor (M-CSF) and granulocyte-macrophage colony stimulating factor (GM-CSF) (Ross 1999). Exposure to these molecules permits macrophages to survive in vitro and possibly to multiply within lesions. If this chronic inflammatory response is unabated and excessive, it can result in an aortic valve lesion, similar to an atherosclerotic plaque, and ectopic calcification. However, calcification may be inhibited by the presence of certain molecules including osteopontin (OPN) (Steitz et al. 2002) and high-density lipoprotein (Parhami et al. 2002).

The ideal TE heart valve should elicit no inflammatory response. The aim of this study was to further characterize the in vitro cellular response of VICs to mechanical forces to ensure that preconditioning of TE valves did not render them susceptible to lesion formation. Valvular lesion formation is analogous to the atherosclerotic process (Mohler 2004) and it is the continual expression of MCP-1, VCAM-1, GM-CSF and OPN molecules by vascular smooth muscle cells that controls lesion formation and calcification in blood vessels (Dzau et al. 2002). Hence, the differential expression of these genes in VICs at varying strains was studied to assess the potential development of valvular lesions in TE valves.

2 Materials and methods

2.1 Cell isolation and culture

Porcine hearts were kindly donated by the Meat Lab at Mississippi State University. Aortic valves were obtained from adult female pigs within 30 min of slaughter and transported to the laboratory in ice-cold Dulbecco's Phosphate Buffered Saline (PBS; Sigma, St. Louis, MO). Porcine aortic VIC were isolated as previously described (Butcher and Nerem 2004). In brief, after removal of the endothelium, leaflets underwent enzymatic digestion with collagenase II solution (~300 U/ml; Worthington Biochemical Corp., Lakewood, NJ) for 6 h at 37°C and 5% CO_2 with gentle agitation. The resulting cell solution was centrifuged for 5 min at 1,000 rpm and the pellet was rinsed twice with PBS before seeding into a 75 ml tissue culture flask with Dulbecco's Modified Eagle Medium (DMEM; Sigma) supplemented with 10% Fetal Bovine Serum (FBS; Hyclone, Logan, UT) and 1% Anti-biotic/Anti-mycotic solution (ABAM; Sigma). Cells were maintained at 37°C in a 5% CO_2 humidified environment with medium changes every 2 days.

2.2 Cyclic straining of cultured cells

Confluent VIC's were harvested at passage 1 by treatment with Trypsin-EDTA (Sigma), and cells were seeded into Bioflex® flexible collagen type I culture plates (Flexercell International, Hillsboro, NC) at a density of 10^6 cells/well with 3ml DMEM supplemented with 10% FBS and 1% ABAM. When cells reached 80% confluence, cell media was removed from each well and cells were rinsed twice with sterile PBS. Cells were then incubated with DMEM supplemented with 0.1% FBS for 24 h to suppress cell cycle. For gene expression studies, cells were subjected to a defined cyclic strain for 2 h, at a frequency of 1 Hz (equivalent to 60 bpm), using a Flexercell® 4000T Tension Plus System (Flexercell International), housed in a 37°C incubator with 5% CO_2. The duration correlates to previous studies that have examined changes in gene expression in VICs (Warnock et al. 2006). Protein expression was evaluated in cells that were stretched at 15% for 2 and 24 h. The Flexercell Tension Plus System is a computer-regulated bioreactor that simulates biological strain conditions using negative vacuum pressure to stretch the flexible membrane over a loading post and thus deforming cells cultured on the flexible growth surface. A pressure transducer enables the system to closely monitor and control the degree of stretch. The strains used in this study were 5, 10, 15 and 20%. The applied cyclic strains were chosen to represent a range that would mimic physiological (15% strain) and pathological strain conditions (Balachandran et al. 2006). Control cultures were incubated under static conditions in Bioflex® flexible collagen type I culture plates.

2.3 Real time polymerase chain reaction

Semi-quantitative reverse transcriptase polymerase chain reaction (RT PCR) was done to measure the relative change in mRNA expression of Monocyte Chemotactic Protein 1 (MCP-1), Vascular Cell Adhesion Molecule 1 (VCAM-1), Granulocyte-Macrophage Colony Stimulating Factor (GM-CSF) and Osteopontin (OPN). Primers were designed using Primer3 software (Rozen and Skaletsky 2000). Sequences were selected that crossed intron/exon boundaries to ensure the elimination genomic DNA. Specific details of the primer sequences are given in Table 1. Immediately after cyclic straining, total RNA was isolated for gene expression analysis using the RNeasy Mini Kit (Qiagen, Valencia, CA), according to the manufacturer's instructions. RNA integrity and quantity was measured using a Nanodrop ND-1000 Spectrophotometer (Thermo Fisher Scientific Inc., Wilmington, DE). RT PCR was done using the SuperScript™ III

Table 1 Primer sequences used for RT PCR

Gene	Primer sequence	GenBank accession number
MCP-1	5′-GTCCTTGCCCAGCCAGATG-3′ (F)	Z48479
	5′-CGATGGTCTTGAAGATCACTGCT-3′ (R)	
OPN	5′-GGTCTATGGACTGAGGTCAAAATCTA-3′ (F)	NM214023
	5′-TCCGAGGAAATAGTATTCTGTGGC-3′ (R)	
VCAM-1	5′-GAGATATGGTGACTGGGGTGGTG-3′ (F)	NM213891
	5′-GAACAAACAACATCATAAAAA-3′ (R)	
GM-CSF	5′-GCTGTGATGAATGAAACCGTAGAC-3′ (F)	NM214118
	5′-TGGGTTTCACAGGAAGTTTCCTC-3′ (R)	
18s	5′-CGGAGAGGGAGCCTGAGAAA-3′(F)	AY265350
	5′-CGGGTCGGGAGTGGGTAAT-3′(R)	

Platinum® SYBR® Green One-Step qRT-PCR Kit (Invitrogen Life Technologies, Carlsbad, CA). A master mix was created using 0.25 μl SYBR® Green One-Step Enzyme Mix, 6.25 μl 2X SYBR® Green Reaction Mix, 0.25 μl of forward and reverse primers and RNase/DNase free distilled water to give a final volume of 11.5 μl per sample. The master mix was pipetted into a 96-well PCR plate and 1 μl of total RNA for each sample (between 250 and 750 ng) was added, giving a final reaction volume of 12.5 μl. cDNA synthesis and PCR amplification was performed using the following steps: 50°C for 30 mins then the reaction mixture was heated to 95°C for 5 min; a 45 cycle two-step PCR was performed consisting of 95°C for 15 s followed by 1 min at 60°C. Reactions were carried out using an i-Cycler Thermal Cycler (Bio-Rad Laboratories, Hercules, CA). Following amplification a melt curve was generated that confirmed primer specificity and the absence of primer-dimers.

2.4 Confocal laser scanning microscopy

Confocal laser scanning microscopy (CLSM) was used to observe protein expression after 2 h. The proteins of interest were VCAM-1, MCP-1 and GM-CSF. OPN protein expression was not assessed as no changes in gene expression were observed. Additionally, pSMAD 2/3 and IκB were evaluated to elucidate the possible signaling mechanisms induced by cyclic strain. These molecules were observed after 2 and 24 h. Upon completion of the cyclic stretching or static incubation experiments, Bioflex collagen membranes were washed twice in PBS for 5 min each at 37°C. Cells were fixed at 4°C in 4% paraformaldehyde (Electron Microscopy Sciences). Permeabilization and removal of autofluorescence from fixation was performed by rinsing for 30 min with agitation with PBS supplemented with 0.01M glycine and 0.1% Triton-X (both Sigma) at room temperature. The membranes were then washed with PBS with 5% bovine serum albumin (bovine serum albumin, Sigma). Non-specific antibody binding was prevented by incubation in 1% normal goat serum (NGS, sigma) in PBS supplemented with 1% BSA. Membranes were incubated in primary antibody dilutions (VCAM-1 1:100 FITC-Conjugated Mouse Anti-Human $IgG_{2\alpha}$, MCP-1 FITC-Conjugated Mouse Anti-Human $IgG_{2\beta}$ 1:100, 1:100 GM-CSF Mouse Anti-Porcine IgG1; All from R&D Systems, Minneapolis, MN), I κ-Bα [pS32, NOT pS36] (1:1,000 Rabbit Anti-Human [100% homologous to porcine], Biosource, Camarillo, CA, pSMAD 2/3 (Ser 423/425) 1:100, Polyclonal Rabbit Anti-Human IgG (Santa Cruz Biotechnology, Santa Cruz, CA) in PBS with 1% BSA) on with slow agitation at 4°C. Cells were then rinsed twice for 15 min in PBS with 1% BSA. Cells were then blocked for non-specific staining of secondary antibodies with PBS with 1% NGS and 1% BSA. Secondary antibodies (Alexa Fluor 488 goat anti- mouse IgG1 and Alexa Fluor 488 goat anti-rabbit IgG, Invitrogen, 1:200 in PBS with 1% BSA) were incubated for 2 h at 37°C for samples with unconjugated primary antibodies. A 15 min rinse in PBS with 1% BSA was carried out followed by a rinse in PBS. Rhodamine Phalloidin (Invitrogen 3 μg/ml) incubation for 1 h at 37°C with agitation was then performed. Cells underwent a final rinse in PBS twice for 15 min. Membranes were cut out of the Bioflex plates with a razor, plated on a microscope slide and a drop (∼25 μl) of Vectashield Fluorescent Mounting Medium with DAPI (Vector Laboratories, Burlingame, CA) was allowed to spread over the membrane. A 1.5 mm glass coverslip was carefully applied to prevent air bubbles and the membranes were mounted on coverslides and sealed with clear acrylic nailpolish.

A Zeiss LSM 510 confocal laser scanning microscope was used for this study. Cell nuclei, stained with DAPI, were visualized with a 405-30 Diode Laser at 25% transmission in the blue channel. F-actin in the red channel was visualized with a HeNe543 Laser at 20% transmission. Target proteins were visualized in the green channel by exciting AF 488 secondary

antibodies or FITC-conjugated primary antibodies with an Argon-2 laser at 488 nm excitation. A 20X air or 40X oil objective was used when adhesion and chemotactic molecules were visualized. For the intracellular location of IκBα, 63X oil immersion magnification was used. For image acquisition, identical laser powers were used for cell nuclei and F-actin, with adjustments made for varied magnifications. Gain and offset were set sequentially by first adjusting gain to have a minimal population of saturated pixels, and the offset was increased to give a black background. This results in pixel values in each channel to be separated easily in post-processing and reduces cross-over between channels. The laser power for Alexa Fluor conjugated antibodies was set higher than FITC-conjugated Abs due to the increased photostability of the AF molecules. FITC Abs (VCAM-1, MCP-1) were visualized with special care taken to avoid loss of fluorescence. Single images were taken at 20X and 40X, and Z-stacks were taken at 63X at 1 μm intervals through the depth of the cell to visualize IκB α location. Zeiss LSM Image Browser software was used to make a maximum intensity projection of Z-stacks.

Adobe Photoshop CS2 (Adobe Systems Inc., San Jose, CA) was used to process images according to guidelines from the Microscopy Association of America (John Mackenzie, NC State, Confocal Microscopy Workshop). This method was used to avoid data manipulation from conventional "brightness/contrast" methods that have become abundantly abused. Light and dark levels were set using the histogram of pixel values of individual channels. Light levels, or saturation point, a level of 255 in an 8-bit image or 4,095 in a 12-bit image, were set to the first discernible pixels in each channel individually. This assured that the brightest pixel level was set to the saturation point. This was a process known as histogram stretching, a method that spreads data from each channel across the 256 or 4,096 level spectrum, enhancing contrast of the data, while taking care not to over-represent bright spots, or have data on the dark side of the spectrum set to black artificially. Next, gamma levels were set sequentially in the red, blue, and green channels. Identical gamma levels were used for the green channel to give a proper comparison between images.

2.5 Data analysis

At least four experiments were run for each condition. The level of gene expression was calculated as $2^{-\Delta Ct}$, assuming 100% PCR efficiency. ΔCt was the difference in cycle threshold between the house keeping gene, 18s, and the gene of interest. Results for RT PCR are reported as mean ± 95% confidence interval. One-way analysis of variance was used to compare differences between groups; all statistical analyses were accomplished using SAS analysis software. A p value of 0.05 or less was considered significant.

3 Results

Differential gene expression was measured using RT PCR. The data presented in Figs. 1, 2, 3 and 4 show the relative levels of mRNA expression for MCP-1, VCAM-1, GM-CSF and OPN, respectively. Expression of MCP-1, VCAM-1 and GM-CSF was significantly higher in static cultures when compared to cells that were exposed to strain. When cells were exposed to cyclic strain, MCP-1 expression did not change significantly based on the amount of applied cyclic strain (Fig. 1). In contrast, VCAM-1 gene expression was significantly higher in cells strained 5 and 10% when compared to cells strained 15 or 20% (Fig. 2). Furthermore, GM-CSF expression was significantly higher in 5 and 20% than in 10 or 15%. There was no significant difference between 5 and 20% (Fig. 3). This suggests that the strain magnitude may be a determining factor in the level of VCAM-1 and GM-CSF gene expression. Unlike the other genes examined, OPN expression did not show any significant difference

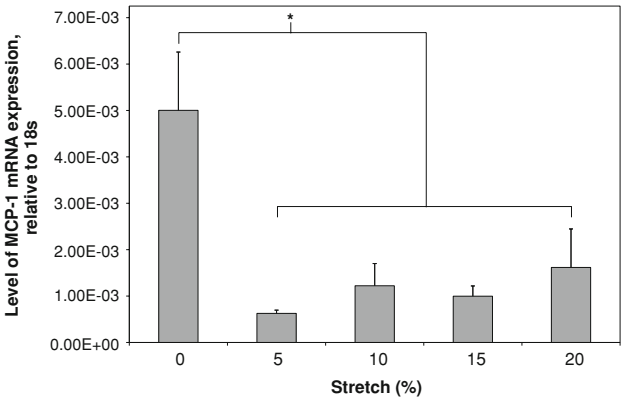

Fig. 1 Level of MCP-1 mRNA expression, relative to 18s, in VICs exposed to cyclic strain for 2 h. *Bars* represent mean values + 95% confidence interval; $n = 4$. $^*p < 0.05$

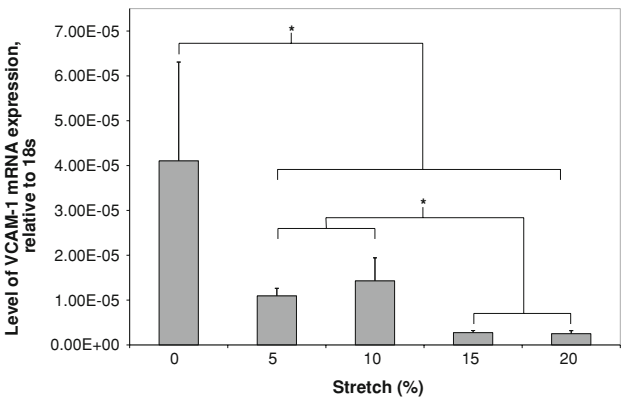

Fig. 2 Level of VCAM-1 mRNA expression, relative to 18s, in VICs exposed to cyclic strain for 2 h. *Bars* represent mean values + 95% confidence interval; $n = 4$. $^*p < 0.05$

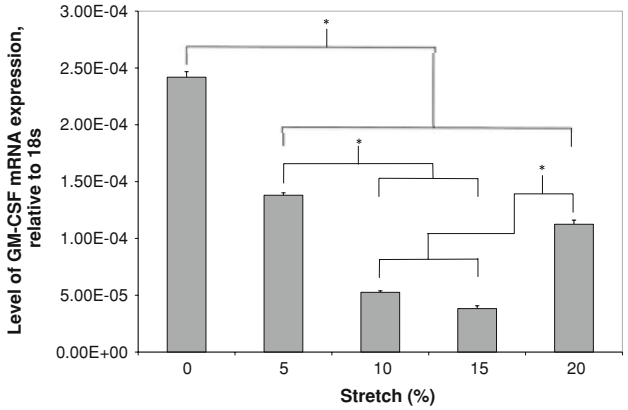

Fig. 3 Level of GM-CSF mRNA expression, relative to 18s, in VICs exposed to cyclic strain for 2 h. *Bars* represent mean values + 95% confidence interval; $n = 4$. $^*p < 0.05$

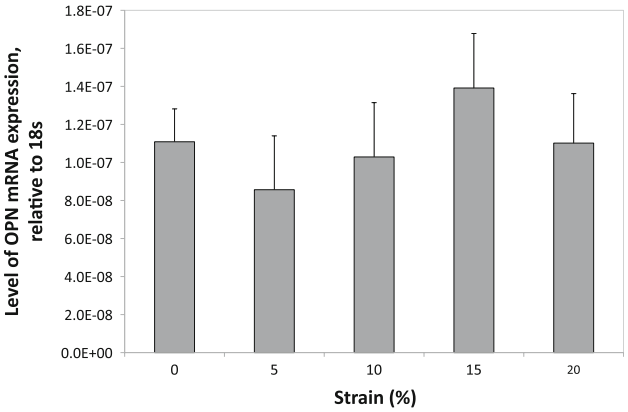

Fig. 4 Level of OPN mRNA expression, relative to 18s, in VICs exposed to cyclic strain for 2 h. *Bars* represent mean values + 95% confidence interval; $n = 4$. $^*p < 0.05$

regardless of strain condition (Fig. 4). The cycle threshold for 18s did not vary between different testing conditions.

To verify the gene expression data, CLSM was used to visualize protein expression. As can be seen in Fig. 5, VCAM-1 and MCP-1 were not detected in stretched cultures, although low levels were present in static controls. GM-CSF could be detected in both stretched and static cultures but levels were higher in the control group. This was consistent with the mRNA data. OPN protein expression was not visualized as no significant changes in mRNA level were detected by RT-PCR. To elucidate the mechanisms responsible for changes in mRNA, pSMAD 2/3 and IκB α expression was assessed. As shown in Fig. 6, no discernable differences in expression could be detected after 2 h. However, after 24 h pSMAD 2/3 was higher in stretched cultures. Also, IκBα was diffused throughout the cytoplasm after 24 h of 15% stretch, whereas it remained concentrated in the nucleus after 24 h static incubation.

4 Discussion

Tissue based artificial heart valves offer great promise, especially for pediatric patients where the valve grows with the host, alleviating the need for repeat surgery. The remodeling capacity of the valve is made possible through the presence of a viable cell population. In vivo recellularization of decellularized allograft valve conduits does occur but is focally limited to regions of the arterial wall and cusp base (Hilbert et al. 2004). Therefore, in vitro seeding prior to implantation is the more attractive method of introducing a cell population, regardless of the substrate. A fundamental understanding of cell behavior is necessary to predict and prevent adverse reactions and potential failure of the valve after implantation. Once the valve is implanted it will be exposed to a demanding and highly complex mechanical environment. Previous studies have demonstrated that this environment is important in maintaining homeostasis in the aortic valve and the absence of these forces causes structural and phenotypical changes in the tissue (Balachandran et al. 2006; Konduri et al. 2005; Weston and Yoganathan 2001; Xing et al. 2004). Additionally, mechanical pre-conditioning of tissue engineered valves improves microstructure, mechanical properties, and extracellular matrix formation (Hoerstrup et al. 2000; Ku et al. 2006). Hence, the appropriate mechanical cues are beneficial to functional valve development and remodeling. As several inflammatory molecules are known to be mechanosensitive, this study aimed to evaluate the inflammatory potential of VICs exposed to mechanical deformation in the form of cyclic strain.

The results of this study demonstrate that cyclic strain was able to lower the amount of MCP-1, VCAM-1 and GM-CSF mRNA within a 2-h period. The absence of cyclic strain does not represent physiological conditions and the cells recognized this as an abnormal state. The increased level of MCP-1, VCAM-1 and GM-CSF gene expression after 2 h, and the localization of IκBα in the nucleus after 24 h, may be indicative of an injury response. However, when cyclic strain was applied to cells, gene expression levels dropped and IκBα could be observed throughout the cytoplasm. The magnitude of cyclic strain did not have any effect on the level of MCP-1 expression. Conversely, VCAM-1 and GM-CSF expression did show some reliance on strain magnitude. VCAM-1 expression was significantly higher at 5 and 10% strain compared to 15 and 20% strain, whereas GM-CSF expression was significantly higher at 5 and 20% strain compared to 10 or 15% strain. In vivo analysis of leaflet strain has shown that leaflet length decreases between diastole and systole by 10.6 and 23.5% in the circumferential and radial directions, respectively (Thubrikar et al. 1980, 1986). Hence, the 15% strain condition may be the closest representation of the normal physiological in vivo state. It appears that deviations from this strain may instigate an injury response by increas-

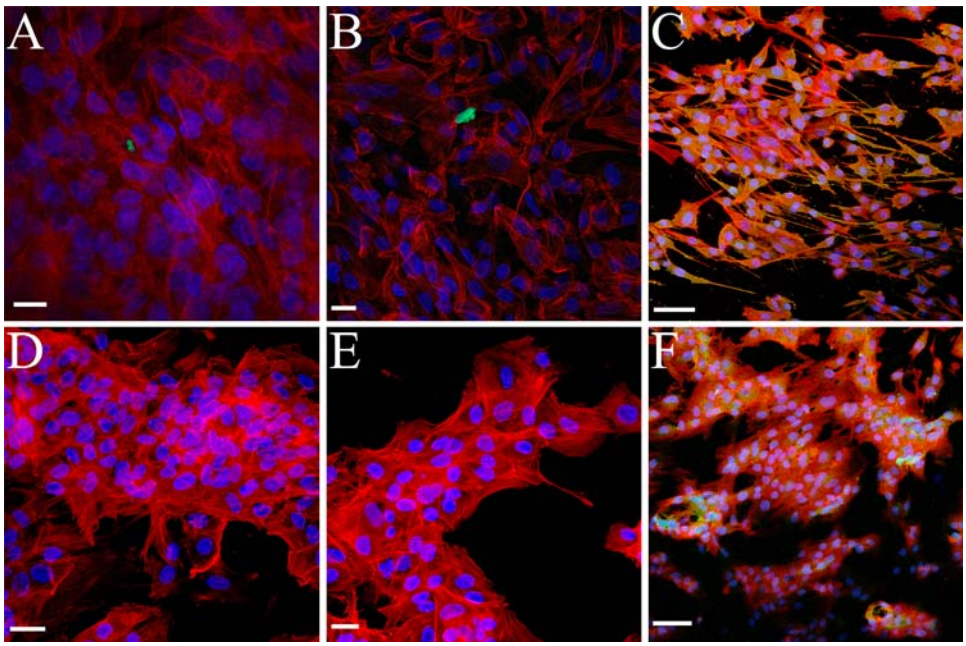

Fig. 5 Confocal laser scanning microscopy images of cells exposed to static (**a**–**c**) or 15% strain (**d**–**f**) conditions. *Blue* cell nuclei, *red* f-actin, *green* MCP-1 (**a**, **d**), VCAM-1 (**b**, **e**), GM-CSF (**c**, **f**). *Scale bars* represent 10 μm (**a**) and 20 μm (**b**–**f**)

ing levels of pro-inflammatory mRNA. This hypothesis is supported further by previous work examining the response of AVEC to cyclic strain. It was shown that VCAM-1, ICAM-1 and E-selectin protein expression was significantly higher in cells exposed to 5 and 20% strain compared to 10% strain (Metzler et al. 2008).

The decrease in mRNA could be attributed to numerous events. Cyclic strain could be responsible for inhibition of the promoter, thus decreasing mRNA transcription; alternatively, mRNA stability could be decreased leading to accelerated turnover. To elucidate the possible mechanism IκB α and pSMAD 2/3 protein expression was examined by CLSM. After 2 h there was no discernable difference in expression levels; however, after 24 h there was a noticeable difference in the expression and spatial distribution of these molecules. Expression of pSMAD 2/3 was significantly higher in stretched cultures, compared to static controls; IκB α was concentrated in the nucleus of static cells but diffused throughout the cytoplasm of cells stretched 15%.

Activated TGFβ/activin receptors phosphorylate SMAD 2 or SMAD 3. The phosphorylated SMAD oligomerizes with SMAD 4 and translocates to the nucleus were it can activate target genes. pSMAD is dephosphorylated in the nucleus and exported to the cytoplasm. Therefore, the high level of pSMAD expression in stretched cells shows that TGFβ was present, presumably being secreted by cells, as it was not present in the culture medium. In adult cells, TGFβ is involved in several processes including, but not limited to, tissue repair and immune regulation. In the context of heart valve tissue engineering, TGFβ1 has been proven to transform fibroblasts into myofibroblasts and consequently upregulate collagen type-1 and TNC expression (Narine et al. 2004). Other studies have shown that TGFβ increases the ability of VICs to rapidly contract free floating collagen gels (Merryman et al. 2007), and significant increases in DNA content and more organized tissue development with pronounced tissue formation with cells seeded on to PGA coated with P4HB (Fu et al. 2004). However, although TGFβ expression may be beneficial to the developing TEHV, excessive expression in an implanted valve may lead to over elaboration of matrix proteins and could result in abnormal valve architecture and fibrosis.

NFκB proteins are central to inflammatory and immune responses in cells. They are held inactive in the cytoplasm by IκB; signals that release NFκB do so by phosphorylating IκB. NFκB translocates to the nucleus where gene expression is activated. Among the genes regulated by NFκB is IκB, which moves to the cytoplasm and binds to NFκB, blocking its action and creating a negative feedback loop. IκB phosphorylation can be caused by cytokines, such as IL1β and TNFα, but has also been associated with mechanical forces in cardiovascular tissues (Lehoux et al. 2006). Our results show that after 24 h there was an abundance of IκBα in the cytoplasm showing that the NFκB pathway was not activated. In contrast, IκBα was concentrated in the nucleus of static controls; the absence in the cytoplasm indicates that NFκB was unbound and able to move to the nucleus and activate gene expression. A number of cytokines and adhesion molecules can be rapidly induced by NFκB, including MCP-1 and VCAM-1 (Tak and Firestein 2001).

Cyclic strain is intrinsically linked to transvalvular pressure in the aortic valve. Hence, as blood pressure increases, so does the transvalvular pressure during diastole and consequently, so does the leaflet strain. In our previous work, it was

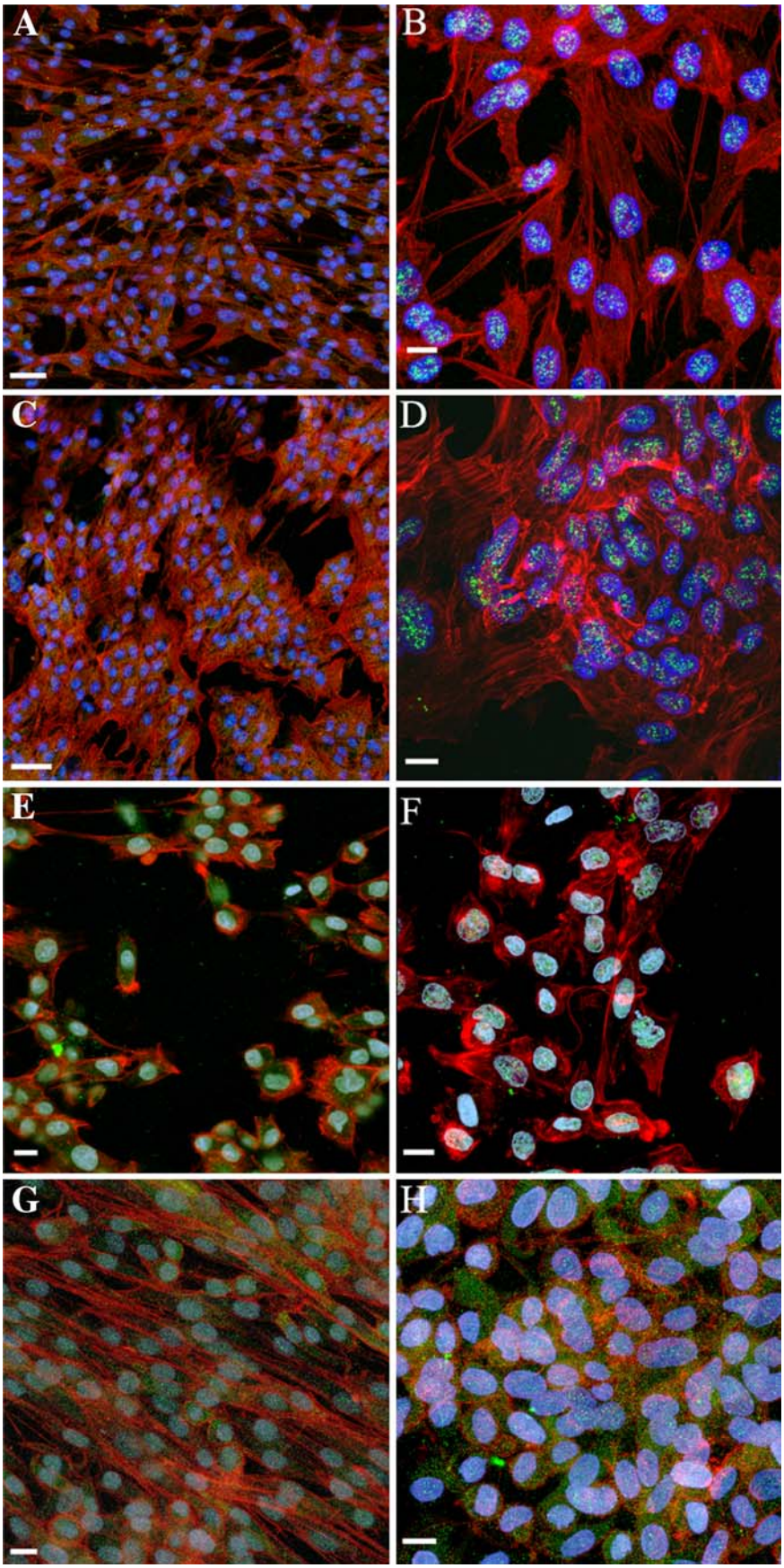

Fig. 6 Confocal laser scanning microscopy images of cells exposed to 0% (**a**, **b**, **e**, **f**) or 15% (**c**, **d**, **g**, **h**) strain for 2 h (**a**–**d**) or 24 h (**e**–**h**). *Blue* cell nuclei, *red* f-actin, *green* pSMAD 2/3 (*left panel*) or IκB α (*right panel*). *Scale bars* represent 50 μm (**a**, **c**), 20 μm (**e**, **g**) or 10 μm (**b**, **d**, **f**, **h**)

shown that elevated cyclic pressure increased expression of VCAM-1, but not MCP-1 or GM-CSF (Warnock et al. 2006). These results, combined with those of the current study, suggest that cyclic strain may be a more important mechanical signal for VICs than pressure. However, cyclic pressure and strain may work synergistically to regulate the expression of VCAM-1 and other pro-inflammatory molecules. Further study is necessary to determine how combined mechanical forces will influence cell activity.

Unlike the pro-inflammatory genes that were examined, OPN expression was not significantly altered between any of the test conditions. OPN is known to be a mechanosensitive gene and is expressed in isolated vascular smooth muscle cells (Nilkolovski et al. 2003). Our results show that cyclic strain does not regulate acute OPN expression in VICs. This may demonstrate a molecular difference between valve and vascular cells, where cyclic strain can regulate OPN expression. Alternatively, the lack of differential expression could also be a temporal effect, and the duration of the current experiments may not be sufficient to elicit any change in OPN gene expression. This theory, however, is suspect as pressure has been shown to regulate differential OPN expression within the same time constraints (Warnock et al. 2006). It can be concluded, though, that cyclic pressure is a more potent stimulus for OPN expression in isolated VICs than cyclic strain.

A major limitation of this study was that mechanosensitive gene expression was assessed in isolated cells. Cells naturally exist in a three-dimensional extra-cellular matrix (ECM), comprised of collagen, elastin and glycosaminoglycans. These biomolecules provide structural/mechanical support to the heart valve tissue and can also transmit mechanical signals to cells. In TEHVs, a scaffold material is used to provide the 3-D geometry. These materials can vary from synthetic polymers, such as PGLA and PLA, to natural materials such as fibrin and collagen hydrogels or decellularized valves. Therefore, as the ECM environment is a determinant of the response of VICs to mechanical stimuli, the gene expression profiles obtained in isolated, cultured cells may not be a faithful representation of the in vivo reaction. These preliminary data provide justification for continuing this avenue of research with organ culture to further elucidate how cyclic strain can influence the in vitro development and preconditioning of a TEHV.

In conclusion, cyclic strain lowered VCAM-1, MCP-1 and GM-CSF mRNA in aortic VICs. The optimal cyclic strain magnitude was 15%. Additionally, 15% strain was able to increase pSMAD 2/3 expression and prevent activation of the NFκB pathway. Therefore, preconditioning of TEHVs with 15% cyclic strain will diminish the expression of pro-inflammatory molecules within the device and may contribute to successful implantation.

Acknowledgments The authors greatly acknowledge Juliet Tang, L. Allen Shack, Joel Howard and Christopher Digesu for their technical assistance. This project was funded in part through an internal grant from the Life Science and Biotechnology Institute at Mississippi State University.

References

Balachandran K, Konduri S, Sucosky P, Jo H, Yoganathan AP (2006) An ex vivo study of the biological properties of porcine aortic valves in response to circumferential cyclic stretch. Ann Biomed Eng 34:1655–1665

Butcher JT, Nerem RM (2004) Porcine aortic valve interstitial cells in three-dimensional culture: comparison of phenotype with aortic smooth muscle cells. J Heart Valve Dis 13:478–485 (discussion 485–486)

Butcher JT, Simmons CA, Warnock JN (2008) Mechanobiology of the aortic heart valve. J Heart Valve Dis 17:62–73

Dzau VJ, Braun-Dullaeus RC, Sedding DG (2002) Vascular proliferation and atherosclerosis: new perspectives and therapeutic strategies. Nat Med 8:1249–1256

Fu P, Sodian R, Luders C, Lemke T, Kraemer L, Hubler M, Weng Y, Hoerstrup SP, Meyer R, Hetzer R (2004) Effects of basic fibroblast growth factor and transforming growth factor-beta on maturation of human pediatric aortic cell culture for tissue engineering of cardiovascular structures. ASAIO J 50:9–14

Hilbert SL, Yanagida R, Souza J, Wolfinbarger L, Jones AL, Krueger P, Stearns G, Bert A, Hopkins RA (2004) Prototype anionic detergent technique used to decellularize allograft valve conduits evaluated in the right ventricular outflow tract in sheep. J Heart Valve Dis 13:831–840

Hoerstrup SP, Sodian R, Daebritz S, Wang J, Bacha EA, Martin DP, Moran AM, Guleserian KJ, Sperling JS, Kaushal S, Vacanti JP, Schoen FJ, Mayer JE Jr (2000) Functional living trileaflet heart valves grown in vitro. Circulation 102:III44–III49

Hoerstrup SP, Kadner A, Melnitchouk S, Trojan A, Eid K, Tracy J, Sodian R, Visjager JF, Kolb SA, Grunenfelder J, Zund G, Turina MI (2002) Tissue engineering of functional trileaflet heart valves from human marrow stromal cells. Circulation 106:I143–I150

Konduri S, Xing Y, Warnock JN, He Z, Yoganathan AP (2005) Normal physiological conditions maintain the biological characteristics of porcine aortic heart valves: an ex vivo organ culture study. Ann Biomed Eng 33:1158–1166

Ku CH, Johnson PH, Batten P, Sarathchandra P, Chambers RC, Taylor PM, Yacoub MH, Chester AH (2006) Collagen synthesis by mesenchymal stem cells and aortic valve interstitial cells in response to mechanical stretch. Cardiovasc Res 71:548–556

Lehoux S, Castier Y, Tedgui A (2006) Molecular mechanisms of the vascular responses to haemodynamic forces. J Intern Med 259:381–392

Merryman WD, Liao J, Parekh A, Candiello JE, Lin H, Sacks MS (2007) Differences in tissue-remodeling potential of aortic and pulmonary heart valve interstitial cells. Tissue Eng 13:2281–2289

Metzler SA, Pregonero CA, Butcher JT, Burgess SC, Warnock JN (2008) Cyclic strain regulates pro-inflammatory protein expression in porcine aortic valve endothelial cells. J Heart Valve Dis 17:571–578

Mohler ER III (2004) Mechanisms of aortic valve calcification. Am J Cardiol 94:1396–1402, A6

Narine K, Dewever O, Cathenis K, Mareel M, Van Belleghem Y, Van Nooten G (2004) Transforming growth factor-beta-induced transition of fibroblasts: a model for myofibroblast procurement in tissue valve engineering. J Heart Valve Dis 13:281–289 (discussion 289)

Nikolovski J, Kim BS, Mooney DJ (2003) Cyclic strain inhibits switching of smooth muscle cells to an osteoblast-like phenotype. FASEB J 02-0459fje

Parhami F, Basseri B, Hwang J, Tintut Y, Demer LL (2002) High-density lipoprotein regulates calcification of vascular cells. Circ Res 91:570–576

Ross R (1999) Atherosclerosis—an inflammatory disease. N Engl J Med 340:115–126

Rozen S, Skaletsky HJ (2000) Primer3 on the WWW for general users and for biologist programmers. In: Krawetz S, Misener S Bioinformatics methods and protocols methods in molecular biology. Humana Press, Totowa

Shahi CN, Ghaisas NK, Goggins M, Foley B, Crean P, Kelleher D, Walsh M (1997) Elevated levels of circulating soluble adhesion molecules in patients with nonrheumatic aortic stenosis. Am J Cardiol 79:980–982

Steitz SA, Speer MY, Mckee MD, Liaw L, Almeida M, Yang H, Giachelli CM (2002) Osteopontin inhibits mineral deposition and promotes regression of ectopic calcification. Am J Pathol 161:2035–2046

Tak PP, Firestein GS (2001) NF-kappaB: a key role in inflammatory diseases. J Clin Invest 107:7–11

Thubrikar M, Piepgrass WC, Bosher LP, Nolan SP (1980) The elastic modulus of canine aortic valve leaflets in vivo and in vitro. Circ Res 47:792–800

Thubrikar MJ, Aouad J, Nolan SP (1986) Comparison of the in vivo and in vitro mechanical properties of aortic valve leaflets. J Thorac Cardiovasc Surg 92:29–36

Warnock JN, Burgess SC, Shack A, Yoganathan AP (2006) Differential immediate-early gene responses to elevated pressure in porcine aortic valve interstitial cells. J Heart Valve Dis 15:34–41 (discussion 42)

Weston MW, Yoganathan AP (2001) Biosynthetic activity in heart valve leaflets in response to in vitro flow environments. Ann Biomed Eng 29:752–763

Xing Y, Warnock JN, He Z, Hilbert SL, Yoganathan AP (2004) Cyclic pressure affects the biological properties of porcine aortic valve leaflets in a magnitude and frequency dependent manner. Ann Biomed Eng 32:1461–1470